

interaction, unlike the two observed by Xu and Cafiso. Our terminal methyl- $^+NMe_3$ cross peak is exceedingly weak, unlike that seen in the sonicated system, due in that case presumably to lipid interdigitation or chain bends. The diagonal peaks for the α -, β -, and γ -headgroup peaks are unsplit, owing to equivalence of the two halves of the bilayer. Finally, because our system has much less excess water, loss of magnetization to this large "bath" is attenuated, and we observe cross peaks with HO^2H for $^+NMe_3$ and hydrocarbon chain protons, reflecting, we believe, the presence of substantial amounts of HO^2H in the lipid bilayer.

Conclusions and Future Prospects

We can summarize our conclusions as follows: (1) high-field 1H MASS NMR yields narrow, multilined spectra for many liquid crystalline lipid bilayer systems, from which isotropic chemical shifts can be determined; (2) resolution in 1H MASS is about as good as with sonicated systems, and is much better than with oriented samples; (3) line widths and spin-lattice relaxation times, for individual groups, can be readily measured (T_2 and $T_{1\rho}$ determinations should also be feasible); (4) information on order parameters can (probably) be extracted from the spinning-sideband manifold, without isotopic labeling; (5) two-dimensional (2-D) NMR techniques can probably be used to obtain spatial or connectivity information (via cross-relaxation or scalar coupling effects); (6) strongly dipolar coupled systems, e.g., the gel phase of DMPC, may not yield high-resolution spectra at convenient

spinning rates; (7) data acquisition is at least an order of magnitude faster than with conventional techniques; (8) there is no requirement to subject samples to ultrasonic irradiation; and (9) there is no requirement for isotopic labeling (as with 2H).

In the future, it may be possible to obtain improved resolution, and to use 1H J -coupling information. However, such experiments are expected to be somewhat difficult, since a typical 1H high-resolution specification of 0.5 Hz corresponds to only 0.001 ppm at 500 MHz, a value not met by conventional MASS NMR probes. Thus, some efforts will have to be expended on probe construction, shimming, field-locking, and so forth. In addition, relaxation effects may prohibit some such experiments. Alternatively, various resolution enhancement aids may be applied to improve spectral resolution, since signal-to-noise ratios are high.

The ability to record highly resolved 1H (1- and 2-D) spectra implies that a variety of *heteronuclear* 2-D experiments (involving, for example, 2H , ^{13}C , ^{14}N , ^{15}N , and ^{31}P) may be applied to unsonicated lipid (and biological) membranes. We hope the results presented in this publication spur such activities.

Acknowledgment. We are very grateful to Professor Myer Bloom and Drs. A. Vega and N. Zumbulyadis for their helpful comments on the origin of spinning sidebands in liquid crystalline systems.

Registry No. CHOL, 57-88-5; Na decanoate, 1002-62-6; decanol, 112-30-1; water, 7732-18-5; K oleate, 143-18-0; lecithin, 18194-24-6.

Observation of a Mobile Molybdenum Carbonyl Fragment on γ -Alumina by Solid-State Carbon-13 Nuclear Magnetic Resonance Spectroscopy

Thomas H. Walter, Arthur Thompson, Max Keniry, Sumio Shinoda,[†] Theodore L. Brown, H. S. Gutowsky, and Eric Oldfield*

Contribution from the School of Chemical Sciences, University of Illinois at Urbana-Champaign, 505 South Mathews Avenue, Urbana, Illinois 61801. Received February 4, 1987

Abstract: High-resolution solid-state carbon-13 nuclear magnetic resonance spectroscopic studies of a chemisorbed molybdenum hexacarbonyl fragment on γ -alumina are described. It is shown that chemical shift anisotropy information, obtained by analysis of spinning sideband intensities in magic-angle spinning spectra, can be used to study the mobilities of chemisorbed metal carbonyl fragments. Evidence is presented for very facile rotation of a $Mo(CO)_5(ads)$ species about the surface-Mo bond.

In the past decade there has been growing interest in the preparation of heterogeneous catalysts by reaction of transition metal carbonyl complexes with high surface area metal oxides, such as transitional aluminas and porous silica.¹⁻⁴ In addition to providing novel catalysts, these supported complexes may also afford relatively well-defined surface structures, allowing the identification of important features of heterogeneous catalysts through systematic synthesis and characterization. Unfortunately, in most cases many structural questions remain after characterization by such readily available techniques as infrared spectroscopy, ultraviolet-visible spectroscopy, and temperature-programmed desorption.³ The availability of solid-state carbon-13 nuclear magnetic resonance (NMR) spectroscopic data on these systems has thus been eagerly anticipated.^{3,4} Although only highly mobile physisorbed species could be detected in the earliest ^{13}C NMR studies of supported metal carbonyls,⁵ recent studies using solid-state NMR techniques such as magic-angle spinning (MAS)

and cross polarization (CP) have shown that less mobile chemisorbed species can also be observed.⁶⁻⁸

One of the most extensively studied supported complexes is molybdenum hexacarbonyl on γ -alumina, which has been exam-

(1) Yermakov, Yu. I.; Kuznetsov, B. N.; Zakharov, V. A. *Catalysis by Supported Complexes*; Elsevier: Amsterdam, 1981.

(2) (a) Bailey, D. C.; Langer, S. H. *Chem. Rev.* **1981**, *81*, 109. (b) Basset, J. M.; Choplin, A. *J. Mol. Catal.* **1983**, *21*, 95.

(3) Hartley, F. R. *Supported Metal Complexes*; D. Reidel: Dordrecht, Holland, 1985.

(4) Gates, B. C. In *Metal Clusters*; Moskovits, M., Ed.; Wiley: New York, 1986; p 283.

(5) (a) Ben Taarit, Y.; Wicker, G.; Naccache, C. In *Magnetic Resonance in Colloid and Interface Science*; Fraissard, J. P., Resing, H. A., Eds.; Reidel: Dordrecht, Holland, 1980; p 497. (b) Nagy, J. B.; Van Eenoo, M.; Derouane, E. G.; Vedrine, J. C. *Ibid.*, p 591. (c) Gelin, P.; LeFebvre, F.; Elleuch, B.; Naccache, C.; Ben Taarit, Y. *ACS Symp. Ser.* **1983**, *No. 218*, 455.

(6) Liu, D. K.; Wrighton, M. S.; McKay, D. R.; Maciel, G. E. *Inorg. Chem.* **1984**, *23*, 212.

(7) Toscano, P. J.; Marks, T. J. *Organometallics* **1986**, *5*, 400.

(8) Hanson, B. E.; Wagner, G. W.; Davis, R. J.; Motell, E. *Inorg. Chem.* **1984**, *23*, 1635.

[†] On leave from the Institute of Industrial Science, University of Tokyo, 22-1, Roppongi 7 Chome, Minato-ku Tokyo 106, Japan.

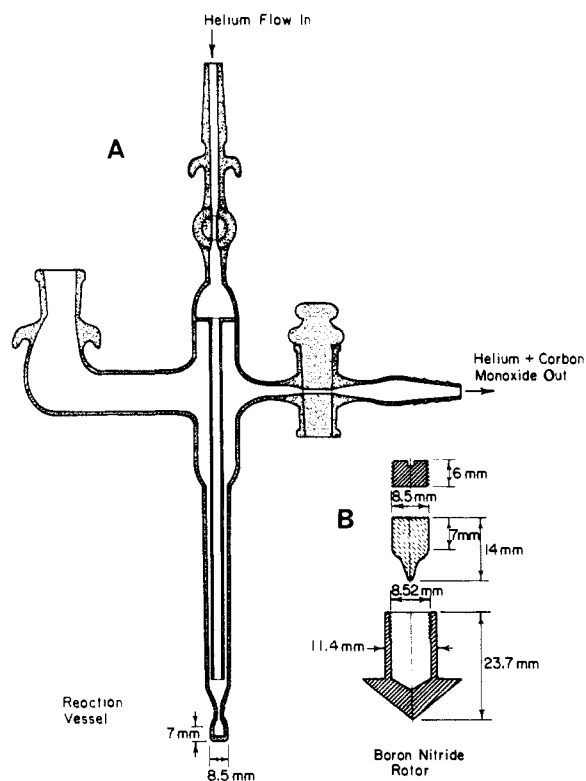


Figure 1. Diagram of (A) the reaction vessel used for calcining the Al_2O_3 and activating the sample, and (B) the sealed ampule and the Andrew-Beams rotor.

ined by temperature-programmed desorption,⁹ infrared spectroscopy,¹⁰ and, most recently, ^{13}C NMR spectroscopy.^{8,11} In one of these studies,¹¹ spectra were recorded under solution NMR conditions, so that only the narrow resonance from physisorbed $\text{Mo}(\text{CO})_6$ could be seen, while in the second study,⁸ the use of CPMAS enabled the observation of resonances from the less mobile, chemisorbed molybdenum carbonyl fragments. We have examined this system using solid-state ^{13}C NMR at high field (8.45 T) in order to achieve greater sensitivity and resolution, and to obtain information on the chemical shift anisotropies of chemisorbed molybdenum carbonyl fragments. We demonstrate in this publication how information on the full shielding tensor of the carbonyl ligand can be used to investigate not only the structures of adsorbed metal carbonyls, but also their mobilities.

Experimental Section

Chemical Aspects. $\text{Mo}(\text{CO})_6$ (Strem, Newburyport, MA) was enriched in ^{13}C by exchange with ^{13}CO (Monsanto Research Corp., Miamisburg, OH) in THF/cyclohexane (1:4) under ultraviolet irradiation and purified by vacuum sublimation. $\text{Mo}(\text{CO})_5(\text{C}_5\text{H}_5\text{N})$ was prepared as described by Koelle¹² and purified by chromatography on alumina. Following the procedure of Burwell and Brenner,⁹ $\text{Mo}(\text{CO})_6/\gamma\text{-Al}_2\text{O}_3$ samples were prepared by impregnating partially dehydroxylated $\gamma\text{-Al}_2\text{O}_3$ with a pentane solution of 60% [^{13}C] $\text{Mo}(\text{CO})_6$ to give a 10 wt % loading. Pentane (American Burdick and Jackson, Muskegon, MI) was dried over CaH_2 and vacuum distilled just prior to use. The $\gamma\text{-Al}_2\text{O}_3$, which was initially prepared by calcining CATAPAL SB boehmite (Conoco Chemicals, Houston, TX) at 753 K for 3 h (surface area after calcination 280 m^2/g), was dehydrated in flowing O_2 for 1 h at 723 K immediately prior to use. Following thermal activation of the $\text{Mo}(\text{CO})_6/\gamma\text{-Al}_2\text{O}_3$ sample in flowing helium (purified by passage through

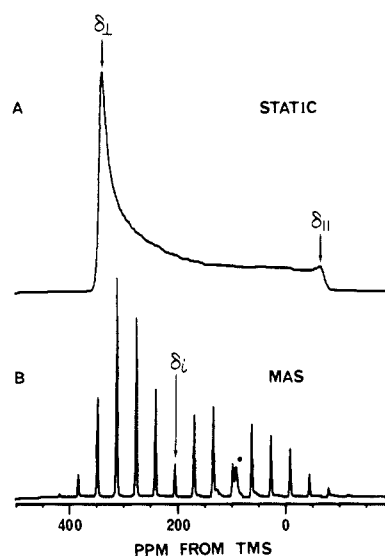


Figure 2. 90.5-MHz ^{13}C NMR spectra of $\text{Mo}(\text{CO})_6$: (A) stationary sample, 65 acquisitions with 200-s recycle time; (B) magic-angle spinning at 3.1 kHz, 80 acquisitions with 50-s recycle time (* indicates a resonance from the delrin rotor).

columns of MnO and 4A molecular sieves), the glass ampule in which the sample was prepared (see Figure 1A) was flame sealed to rigorously exclude oxygen and moisture. The sample weight was typically 150 mg.

NMR Spectroscopy. Carbon-13 spectra were obtained on FTNMR spectrometers operating at 90.5 and 37.8 MHz, using Oxford Instruments 8.45-T, 89-mm bore or Nalorac 3.52-T, 102-mm bore superconducting solenoid magnets. Nicolet Model 1280 computer systems were used for data acquisition, and Amplifier Research Model 150LA and Henry Radio TEMPO 1002 amplifiers for final radio-frequency pulse generation. Magic-angle spinning NMR spectra at both field strengths were obtained using home-built probes employing spinners of the Andrew-Beams type, with 12-mm rotors made of boron nitride (to avoid background ^{13}C resonances) to hold the sealed ampules (see Figure 1B). Variable-temperature static NMR spectra were obtained using a home-built probe with a gas-flow cryostat constructed such that the only significant thermal contact between the sample and the main body of the probe occurs through the coil. The temperatures reported, which are the gas-flow temperatures measured ca. 1 cm from the sample, were measured using either a Doric Trendicator with a copper-constantan thermocouple (273–77 K) or a calibrated¹³ 560- Ω , $1/4$ -W Allen-Bradley carbon resistor (77–4 K). The spectra shown here were obtained without proton decoupling, using 90° pulse excitation (typically 5–10 μs) for MAS experiments and a Hahn echo pulse sequence for static experiments. Spin-lattice relaxation times were estimated using the saturating comb saturation-recovery method¹⁴ to be ca. 60 s for $\text{Mo}(\text{CO})_6$ and ca. 1 s for both the physisorbed $\text{Mo}(\text{CO})_6$ and chemisorbed $\text{Mo}(\text{CO})_5(\text{ads})$ species on $\gamma\text{-Al}_2\text{O}_3$ at room temperature at 90.5 MHz. Chemical shifts are reported in ppm from an external sample of TMS, with low-field (high-frequency), deshielded values being designated as positive, in accord with the IUPAC (δ scale) convention. Principal components of the shielding tensor were approximated from spinning sideband intensities using the graphical method of Herzfeld and Berger,¹⁵ then refined by simulation using a program based on Herzfeld and Berger's numerical results. In all cases the shielding tensor was found to be axially symmetric, within experimental error. The program POWPAT, written by H. S. Story and D. Kline and available from the Quantum Chemistry Program Exchange, was used for simulation of static spectra.

Results and Discussion

The dominant interaction in solid-state ^{13}C NMR spectra of metal carbonyls is the large chemical shift anisotropy (CSA) of the carbonyl ligand.¹⁶ Chemical shift anisotropy refers to the orientation dependence of the chemical shift that arises when the electron distribution around the nucleus under observation has

(9) (a) Brenner, A.; Burwell, R. L. *J. Am. Chem. Soc.* **1975**, *97*, 2565. (b) Burwell, R. L.; Brenner, A. *J. Mol. Catal.* **1975/76**, *1*, 77. (c) Brenner, A.; Burwell, R. L. *J. Catal.* **1978**, *52*, 353.

(10) (a) Howe, R. F.; Davidson, D. E.; Whan, D. A. *J. Chem. Soc., Faraday Trans.* **1972**, *68*, 2266. (b) Howe, R. F. *Inorg. Chem.* **1976**, *15*, 486. (c) Laniecki, M.; Burwell, R. L. *J. Colloid Interface Sci.* **1980**, *75*, 95. (d) Kazusaka, A.; Howe, R. F. *J. Mol. Catal.* **1980**, *9*, 183.

(11) Shirley, W. M.; McGarvey, B. R.; Maiti, B.; Brenner, A.; Cichowlas, A. *J. Mol. Catal.* **1985**, *29*, 259.

(12) Koelle, U. *J. Organomet. Chem.* **1977**, *133*, 53.

(13) Anderson, A. C. In *Temperature, Its Measurement and Control in Science and Industry*; Plumb, H. H., Ed.; Instrument Society of America: Pittsburgh, PA, 1972; Vol. 4, p 773.

(14) Fukushima, E.; Roeder, S. B. W. *Experimental Pulse NMR*, Addison-Wesley: Reading, MA, 1981; pp 174–176.

(15) Herzfeld, J.; Berger, A. E. *J. Chem. Phys.* **1980**, *73*, 6021.

(16) Gleeson, J. W.; Vaughan, R. W. *J. Chem. Phys.* **1983**, *78*, 5384.

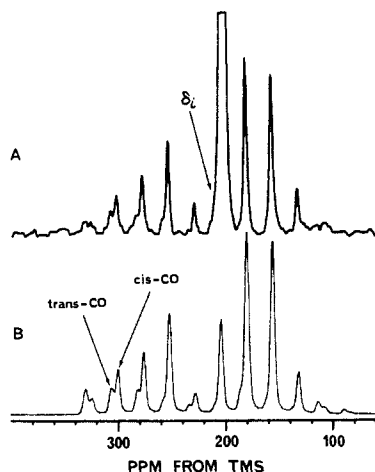


Figure 3. (a) 90.5-MHz magic-angle spinning ^{13}C NMR spectrum of $\text{Mo}(\text{CO})_6/\gamma\text{-Al}_2\text{O}_3$ activated at 100°C for 1 h; spun at 2.2 kHz, 1580 acquisitions, 5-s recycle. The intense resonance at 201 ppm has been truncated to emphasize the weaker $\text{Mo}(\text{CO})_5(\text{ads})$ resonances. (b) Simulation of $\text{Mo}(\text{CO})_5(\text{ads})$ resonances using two components: (i) $\delta_{\perp} = 144$ ppm, $\delta_{\parallel} = 324$ ppm, relative intensity 4.0; (ii) $\delta_{\perp} = 344$ ppm, $\delta_{\parallel} = -58$ ppm, relative intensity 1.0; spinning speed 2.2 kHz.

less than tetrahedral symmetry.¹⁷ The complete chemical shift interaction is described by a second-rank tensor δ , which can be partially characterized by its three principal components, δ_{11} , δ_{22} , and δ_{33} , the average of which is the chemical shift observed in solution NMR (excluding solid-state shifts), termed the isotropic chemical shift (δ_i):

$$\delta_i = \frac{1}{3}(\delta_{11} + \delta_{22} + \delta_{33})$$

When δ is axially symmetric, as is generally the case for carbonyl carbons,¹⁶ two of the principal components are degenerate, leaving only two unique components, designated δ_{\perp} ($= \delta_{11} = \delta_{22}$) and δ_{\parallel} ($= \delta_{33}$). In polycrystalline samples, chemical shift anisotropy gives rise to characteristic line shapes (CSA powder patterns), from which δ_{\perp} and δ_{\parallel} can be obtained, as illustrated in Figure 2A for $\text{Mo}(\text{CO})_6$. The width of the powder pattern, known as the shielding anisotropy ($\Delta\delta$), is given by:

$$\Delta\delta = \delta_{33} - \frac{1}{2}(\delta_{22} + \delta_{11}) = \delta_{\parallel} - \delta_{\perp}$$

where the convention $|\delta_{33} - \delta_{\parallel}| \geq |\delta_{11} - \delta_{\parallel}| \geq |\delta_{22} - \delta_{\parallel}|$ has been used. With magic-angle spinning at a spinning frequency greater than $\Delta\delta$, a single narrow resonance at the isotropic chemical shift would be observed. However, at the high field strength used in this work, this would require speeds in excess of 15 kHz, while the current limit is ca. 5 kHz, for large samples. Thus, we are operating here in the slow spinning regime,¹⁸ where the CSA powder pattern is broken up into a series of narrow spinning sidebands located at multiples of the spinning frequency on either side of δ_i , as illustrated in Figure 2B for $\text{Mo}(\text{CO})_6$. The centerband resonance in such a spinning sideband array is readily identified by changing the spinning speed and locating the peak whose position is unchanged. It has been shown¹⁵ that the relative intensities of the spinning sidebands are related to the three principal components of the shielding tensor, so that in this regime both high-resolution (δ_i) and solid-state (δ_{11} , δ_{22} , δ_{33}) information can be obtained simultaneously. The shielding anisotropy is useful not only for making peak assignments, but can also provide detailed information on dynamics, since rapid molecular motion may partially or completely average the CSA.¹⁹

We show in Figure 3A the ^{13}C MAS NMR spectrum of a $\text{Mo}(\text{CO})_6/\gamma\text{-Al}_2\text{O}_3$ sample activated at 100°C for 1 h. In contrast to the results of Brenner and Burwell,⁹ we obtain only partial conversion of $\text{Mo}(\text{CO})_6$ to chemisorbed species under these ac-

Table I. Principal Components, Isotropic Values, and Anisotropies of the ^{13}C Shielding Tensors for $\text{Mo}(\text{CO})_6$, $\text{Mo}(\text{CO})_5(\text{C}_5\text{H}_5\text{N})$, and $\text{Mo}(\text{CO})_5(\text{ads})^a$

sample	δ_{\parallel}^b	δ_{\perp}^c	δ_i^c	$\Delta\delta^d$
$\text{Mo}(\text{CO})_6$	201	338	-72	-410
		$(343 \pm 15)^e$	(-75 ± 15)	(-417 ± 30)
$\text{Mo}(\text{CO})_5(\text{C}_5\text{H}_5\text{N})$				
cis CO	207	338	-54	-392
trans CO	221	355	-48	-403
$\text{Mo}(\text{CO})_5(\text{ads})$				
cis CO	204	144	324	180
trans CO	210	344	-58	-402

^a Values are in ppm, relative to TMS, and were obtained from MAS spectra. ^b Uncertainties are ± 0.5 ppm. ^c Uncertainties are ± 5 ppm. ^d Calculated from $\Delta\delta = \delta_{\parallel} - \delta_{\perp}$. ^e Values reported by Gleeson and Vaughan, ref 16.

tivation conditions, presumably because of gas-flow restrictions in our reaction vessel. The intense, narrow (25 Hz full-width at half-height, fwhh) resonance at 201 ppm has been assigned^{8,11} to physisorbed $\text{Mo}(\text{CO})_6$. The absence of spinning sidebands for this resonance indicates that the chemical shift anisotropy of physisorbed $\text{Mo}(\text{CO})_6$ is completely averaged, as a result of rapid isotropic reorientation. In addition to this intense resonance, there are a series of broad (250-Hz fwhh), weaker peaks that can be assigned, on the basis of spectra obtained at different spinning speeds, to spinning sideband arrays from two distinct components. The isotropic chemical shifts of these components are 204 and 210 ppm, with the centerbands being obscured by the wings of the intense physisorbed $\text{Mo}(\text{CO})_6$ resonance. We believe that these resonances can be assigned to the cis and trans carbonyls, respectively, of a chemisorbed $\text{Mo}(\text{CO})_5(\text{ads})$ species on the basis of agreement with known chemical shifts of molybdenum hexacarbonyl derivatives such as $\text{Mo}(\text{CO})_5\text{PR}_3$ ($\text{R} = \text{OMe}, \text{OEt}, \text{Ph}$), which have $\delta_{\text{cis}} \sim 206$ ppm and $\delta_{\text{trans}} \sim 210$ ppm.²⁰ This assignment is also consistent with IR results,¹⁰ which show formation of $\text{Mo}(\text{CO})_5(\text{ads})$ as the initial step in the decomposition of $\text{Mo}(\text{CO})_6$. We note, however, that it is difficult to rule out the possibility that the 210-ppm resonance arises from a $\text{Mo}(\text{CO})_4(\text{ads})$ species present in low abundance. The relative intensities of the two resonances are, however, consistent with the 4:1 ratio required by a $\text{Mo}(\text{CO})_5(\text{ads})$ stoichiometry. Although we have not attempted to measure the relative intensities of the 204- and 210-ppm components by summing the integrated intensities of all their sidebands, we have simulated the experimental spectrum using a program based on the spinning sideband intensity calculations of Herzfeld and Berger.¹⁵ As shown in Figure 3B, a simulation using a 4:1 ratio for the 204- and 210-ppm components is in good agreement with the experimental spectrum. While Hanson et al.⁸ have assigned a resonance at 203 ppm, similar to our 204-ppm resonance, to a $\text{Mo}(\text{CO})_5(\text{ads})$ species, the 210-ppm resonance was not observed in that study, which was carried out at a ^{13}C Larmor frequency of 15 MHz. A possible explanation for this discrepancy is that, contrary to the usual observation²¹ that resolution in solid-state ^{13}C NMR is field independent, we find a significant improvement in resolution for this system at high field. In particular, we have observed that the line width (measured with proton decoupling) of the 204-ppm resonance increases only ca. 50% when the Larmor frequency is increased from 37.8 to 90.5 MHz, representing a 60% resolution improvement. Thus, for these samples, the resolution of chemically shifted resonances increases significantly with field strength, making it advantageous to operate at the highest magnetic field strength possible.

The principal components of the shielding tensors found for the $\text{Mo}(\text{CO})_5(\text{ads})$ resonances are listed in Table I, along with those for $\text{Mo}(\text{CO})_6$ and $\text{Mo}(\text{CO})_5(\text{C}_5\text{H}_5\text{N})$. Comparison of the $\Delta\delta$ values shows that the resonance of the cis carbonyls of the $\text{Mo}(\text{CO})_5(\text{ads})$ species has an anomalously small anisotropy, which

(17) Veeman, W. S. *Prog. NMR Spectrosc.* **1984**, *16*, 193.

(18) Maricq, M. M.; Waugh, J. S. *J. Chem. Phys.* **1979**, *70*, 3300.

(19) Pines, A.; Gibby, M. G.; Waugh, J. S. *J. Chem. Phys.* **1973**, *59*, 569.

(20) Braterman, P. S.; Milne, D. W.; Randall, E. W.; Rosenberg, E. J. *Chem. Soc., Dalton Trans.* **1973**, 1027.

(21) VanderHart, D. L.; Earl, W. L.; Garroway, A. N. *J. Magn. Reson.* **1981**, *44*, 361.

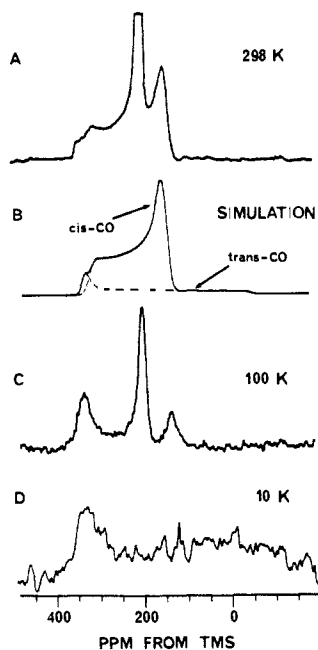


Figure 4. Static 90.5-MHz ^{13}C NMR spectra of $\text{Mo}(\text{CO})_6/\gamma\text{-Al}_2\text{O}_3$ activated at 100 °C for 1 h. (A) Spectrum obtained at 298 K, 8292 acquisitions, 5-s recycle. The intense resonance at 201 ppm has been truncated to emphasize the weaker $\text{Mo}(\text{CO})_5(\text{ads})$ resonances. (B) Simulation of $\text{Mo}(\text{CO})_5(\text{ads})$ powder patterns using same parameters given in Figure 2B cation. (C) Spectrum obtained at 100 K, 312 acquisitions, 5-sec recycle. (D) Spectrum obtained at 10 K, 1008 acquisitions, 2-s recycle.

we attribute to partial averaging by rapid ($\gg 10^5 \text{ s}^{-1}$) anisotropic molecular motion. This hypothesis is supported by a variable-temperature study on this sample, performed without magic-angle spinning because of the difficulty of MAS below 77 K. As shown in Figure 4A, the narrow physisorbed $\text{Mo}(\text{CO})_6$ resonance remains relatively narrow in the static spectrum, while the chemisorbed $\text{Mo}(\text{CO})_5(\text{ads})$ resonances give overlapping CSA powder patterns. The simulation of Figure 4B illustrates how the observed line shape arises from the overlap of the cis and trans carbonyl resonances of the $\text{Mo}(\text{CO})_5(\text{ads})$ species. Note that, because of its low intensity, the only feature we can detect for the 210-ppm component is its low-field singularity at 344 ppm. As shown in Figure 4C, the positions of the singularities of the $\text{Mo}(\text{CO})_5(\text{ads})$ resonances have not changed appreciably at 100 K, while the $\text{Mo}(\text{CO})_6$ peak has broadened noticeably, as previously observed.¹¹ However, at 10 K (Figure 4D) we observe a single broad powder pattern with a ca. 400-ppm anisotropy, as expected for a rigid carbonyl. We believe that this spectrum includes contributions from both the physisorbed and chemisorbed species, but we have been unable to resolve separate features from the two components because of the very inefficient spin-lattice relaxation at this low temperature. The low temperature required to obtain a rigid-lattice spectrum indicates a very low barrier to motion for the chemisorbed $\text{Mo}(\text{CO})_5(\text{ads})$ fragment.

The shielding tensors of the cis and trans carbonyls of the $\text{Mo}(\text{CO})_5(\text{ads})$ species are consistent with an octahedral surface complex undergoing free rotation about the Mo-surface bond (or a fourfold rotational jump), as illustrated in Figure 5. The

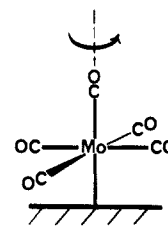


Figure 5. Model proposed to account for the motionally averaged shielding tensor; the rotation axis is indicated.

rotationally averaged shielding anisotropy, $\Delta\delta'$, is related to the rigid-lattice value, $\Delta\delta$, by:

$$\Delta\delta' = \frac{1}{2}(3 \cos^2 \theta - 1)\Delta\delta$$

where θ is the angle between the rotation axis and the direction of δ_{\parallel} , and it has been assumed that the rigid-lattice shielding tensor is axially symmetric.¹⁹ If δ_{\parallel} lies along the CO bond axis, as required by symmetry²² for the trans CO (but not the cis CO) of a $\text{Mo}(\text{CO})_5(\text{ads})$ species with fourfold symmetry, the motionally averaged shielding anisotropy can be used with that for the rigid lattice to calculate θ . Since the spectrum of Figure 3D is not of sufficient quality to allow an accurate determination of the rigid lattice CSA components, we have instead used the values determined for $\text{Mo}(\text{CO})_5(\text{C}_5\text{H}_5\text{N})$, which may be considered to be a model for a rigid $\text{Mo}(\text{CO})_5\text{X}$ species. For the trans CO we find $\theta = 2^\circ$, indicating that the rotation axis nearly coincides with the CO bond axis, as required by the model shown in Figure 5. Note that for this case the shielding tensor is unaffected by the rotation. For the cis carbonyls, we calculate $\theta = 80^\circ$ (or 100° ; both values give the same result), compared with the value of 90° expected from Figure 5. Although this 10° deviation is close to the estimated limit of error in θ ($\pm 5^\circ$), this may indicate that the $\text{Mo}(\text{CO})_5(\text{ads})$ species is slightly distorted from the ideal square-planar structure illustrated in Figure 5, with the cis carbonyls being bent either toward or away from the alumina surface by 10° .

Conclusion

The results presented above indicate that chemisorbed metal carbonyl fragments may undergo restricted motion, as deduced from partial averaging of the ^{13}C chemical shift anisotropy. It is important to note that the particular motion described above has no effect on the isotropic chemical shifts, since it involves exchange between equivalent sites, and hence was not considered in a previous study.⁸ Our results also show that significant improvements in resolution can be achieved for these systems by using high magnetic field strengths. Together, these results conclusively demonstrate the utility of high-field ^{13}C NMR for studying the structures and mobilities of supported metal carbonyl complexes.

Acknowledgment. This work was supported in part by the U.S. National Science Foundation through CHE 83-12331 (T.L.B., S.S.) and the Solid State Chemistry Program (Grants DMR 83-11339 and DMR 86-15206: T.W., A.T., E.O.), and in part by the Mobil Foundation. We thank Michelle Cohn for valuable advice on the very low temperature measurements.

Registry No. $\text{Mo}(\text{CO})_6$, 13939-06-5; Al_2O_3 , 1344-28-1; $\text{Mo}(\text{CO})_5(\text{C}_5\text{H}_5\text{N})$, 14324-76-6.